

A μ - τ -philic Higgs doublet confronted with the muon $g-2$, τ decays and LHC data

Lei Wang¹, Yang Zhang²

¹ *Department of Physics, Yantai University, Yantai 264005, P. R. China*

² *ARC Centre of Excellence for Particle Physics at the Tera-scale,
School of Physics and Astronomy, Monash University,
Melbourne, Victoria 3800, Australia*

Abstract

We propose a two-Higgs-doublet model in which one Higgs doublet has the same interactions with fermions as the SM, and another Higgs doublet only has the μ - τ LFV interactions. Assuming that the Yukawa matrices are real and symmetric, we impose various relevant theoretical and experimental constraints, and find that the excesses of muon $g - 2$ and lepton flavour universality in the τ decays can be simultaneously explained in the region of small mass splittings between the heavy CP-even Higgs and the CP-odd Higgs ($m_A > m_H$). The multi-lepton event searches at the LHC can sizably reduce the mass ranges of extra Higgses, and m_H is required to be larger than 560 GeV.

I. INTRODUCTION

The muon anomalous magnetic moment $g - 2$ has been a long-standing puzzle since the announcement by the E821 experiment in 2001 [1]. There is an almost 3.7σ discrepancy between the experimental value and the prediction of the SM [2]

$$\Delta a_\mu = a_\mu^{exp} - a_\mu^{SM} = (274 \pm 73) \times 10^{-11}. \quad (1)$$

The lepton flavor universality (LFU) in the τ decays is an excellent way to probe new physics. The HFAG collaboration reported three ratios from pure leptonic processes, and two ratios from semi-hadronic processes, $\tau \rightarrow \pi/K\nu$ and $\pi/K \rightarrow \mu\nu$ [3]

$$\begin{aligned} \left(\frac{g_\tau}{g_\mu}\right) &= 1.0011 \pm 0.0015, & \left(\frac{g_\tau}{g_e}\right) &= 1.0029 \pm 0.0015, \\ \left(\frac{g_\mu}{g_e}\right) &= 1.0018 \pm 0.0014, & \left(\frac{g_\tau}{g_\mu}\right)_\pi &= 0.9963 \pm 0.0027, \\ \left(\frac{g_\tau}{g_\mu}\right)_K &= 0.9858 \pm 0.0071, \end{aligned} \quad (2)$$

where the ratios of $\left(\frac{g_\tau}{g_e}\right)$ and $\left(\frac{g_\tau}{g_\mu}\right)_K$ have approximate 2σ discrepancy from the SM.

As a simple extension of the SM, the lepton-specific two-Higgs-doublet model (2HDM) can accommodate the muon $g - 2$ anomaly by the contributions of two-loop Barr-Zee diagrams for a light CP-odd Higgs A and large $\tan\beta$ [4–14]. However, the tree-level diagram mediated by the charged Higgs gives negative contribution to the decay $\tau \rightarrow \mu\nu\bar{\nu}$, which will raise the deviation of the LFU in τ decays [10, 12, 15]. In addition, a scalar with the μ - τ LFV interactions can accommodate the muon $g - 2$ anomaly by the contribution of one-loop diagrams [16–22]. Recently, Ref. [22] showed that the excess of the LFU in τ decays can also be explained by the μ - τ LFV Higgs interactions.

In this work we propose a 2HDM in which one Higgs doublet has the same interactions with fermions as the SM, and another Higgs doublet only has the μ - τ LFV interactions, namely μ - τ -philic Higgs doublet. After imposing the joint constraints from the theory, the precision electroweak data, and the LFU in the Z decays, we examine the parameter space explaining the excesses of muon $g - 2$ and LUF in τ decays. Next, we apply the ATLAS and CMS direct searches at the LHC to constrain the parameter space.

Our work is organized as follows. In Sec. II we recapitulate the model. In Sec. III we discuss the muon $g - 2$, LUF in τ decays, and other relevant constraints, and then use the

direct search limits at the LHC to constrain the model. Finally, we give our conclusion in Sec. IV.

II. THE 2HDM WITH μ - τ -PHILIC HIGGS DOUBLET

An inert Higgs doublet Φ_2 is introduced to the SM under a discrete Z_2 symmetry,

$$\Phi_2 \rightarrow -\Phi_2, \quad (3)$$

while all the SM particles are unchanged. The scalar potential of Φ_2 and Φ_1 is given as

$$\begin{aligned} V = & Y_1(\Phi_1^\dagger \Phi_1) + Y_2(\Phi_2^\dagger \Phi_2) + \frac{\lambda_1}{2}(\Phi_1^\dagger \Phi_1)^2 + \frac{\lambda_2}{2}(\Phi_2^\dagger \Phi_2)^2 \\ & + \lambda_3(\Phi_1^\dagger \Phi_1)(\Phi_2^\dagger \Phi_2) + \lambda_4(\Phi_1^\dagger \Phi_2)(\Phi_2^\dagger \Phi_1) \\ & + \left[\frac{\lambda_5}{2}(\Phi_1^\dagger \Phi_2)^2 + \text{h.c.} \right]. \end{aligned} \quad (4)$$

We focus on the CP-conserving case, and all λ_i are real. The two complex scalar doublets can be written as

$$\Phi_1 = \begin{pmatrix} G^+ \\ \frac{1}{\sqrt{2}}(v + h + iG_0) \end{pmatrix}, \quad \Phi_2 = \begin{pmatrix} H^+ \\ \frac{1}{\sqrt{2}}(H + iA) \end{pmatrix}.$$

The Φ_1 field has the vacuum expectation value (VEV) $v=246$ GeV, and the VEV of Φ_2 field is zero. We determine Y_1 by requiring the scalar potential minimization condition.

$$Y_1 = -\frac{1}{2}\lambda_1 v^2. \quad (5)$$

The G^0 and G^\pm are the Nambu-Goldstone bosons which are eaten by the gauge bosons. The H^\pm and A are the mass eigenstates of the charged Higgs boson and CP-odd Higgs boson. Their masses are given as

$$m_{H^\pm}^2 = Y_2 + \frac{\lambda_3}{2}v^2, \quad m_A^2 = m_{H^\pm}^2 + \frac{1}{2}(\lambda_4 - \lambda_5)v^2. \quad (6)$$

The two CP-even Higgses h and H are mass eigenstates, and there is no mixing between them. In this paper, the light CP-even Higgs h is taken as the SM-like Higgs. Their masses are given as

$$m_h^2 = \lambda_1 v^2 \equiv (125 \text{ GeV})^2, \quad m_H^2 = m_A^2 + \lambda_5 v^2. \quad (7)$$

The masses of fermions are obtained from the Yukawa interactions with Φ_1

$$-\mathcal{L} = y_u \overline{Q}_L \tilde{\Phi}_1 u_R + y_d \overline{Q}_L \Phi_1 d_R + y_l \overline{L}_L \Phi_1 e_R + \text{h.c.}, \quad (8)$$

where $Q_L^T = (u_L, d_L)$, $L_L^T = (\nu_L, l_L)$, $\tilde{\Phi}_1 = i\tau_2 \Phi_1^*$, and y_u , y_d and y_l are 3×3 matrices in family space. To obtain μ - τ -philic Higgs doublet, we introduce the Z_2 symmetry-breaking Yukawa interactions of Φ_2 ,

$$-\mathcal{L} = \sqrt{2} \rho_{\mu\tau} \overline{L}_{2L} \Phi_2 \tau_R + \sqrt{2} \rho_{\tau\mu} \overline{L}_{3L} \Phi_2 \mu_R + \text{h.c.} \quad (9)$$

From Eq. (9), we can obtain μ - τ LFV coupling of extra Higgses (H , A , and H^\pm). We assume that the Yukawa matrices of Φ_2 are CP-conserving, that is $\rho_{\mu\tau}$ and $\rho_{\tau\mu}$ are real and $\rho_{\mu\tau} = \rho_{\tau\mu}$.

At the tree-level, the light CP-even Higgs h has the same couplings to fermions and gauge boson as the SM, and the μ - τ LFV coupling of h is absent. The Yukawa couplings of H , A , and H^\pm are μ - τ -philic, and they have no other Yukawa couplings. The neutral Higgses A and H have no couplings to ZZ , WW . In fact, the model can be derived from general 2HDM in Higgs basis by taking specific parameter space.

III. MUON $g - 2$, LUF IN τ DECAYS, LHC DATA, AND RELEVANT CONSTRAINTS

A. Numerical calculations

In our calculations, we take λ_2 , λ_3 , m_h , m_H , m_A and m_{H^\pm} as the input parameters, which can determine the values of λ_1 , λ_5 and λ_4 from Eqs. (6, 7). λ_2 controls the quartic couplings of extra Higgses, and does not affect the observables considered in our paper. Therefore, we simply take $\lambda_2 = \lambda_1$. λ_3 is adjusted to satisfy the theoretical constraints. We fix $m_h = 125$ GeV, and scan over several key parameters in the following ranges:

$$\begin{aligned} 300 \text{ GeV} < m_H < 800 \text{ GeV}, \quad m_H < m_A = m_{H^\pm} < m_H + 200 \text{ GeV}, \\ 0.1 < \rho_{\mu\tau} = \rho_{\tau\mu} \equiv \rho < 1.0. \end{aligned} \quad (10)$$

At the tree-level, the SM-like Higgs has the same couplings to the SM particles as the SM, and no exotic decay mode for such Higgs mass spectrum. The masses of extra Higgses

are beyond the exclusion range of the searches for the neutral and charged Higgs at the LEP. Because the extra Higgses have no couplings to quarks, the bounds from meson observables can be safely neglected.

In our calculation, we consider the following observables and constraints:

- (1) Theoretical constraints and precision electroweak data. The 2HDMC [23] is employed to implement the theoretical constraints from the vacuum stability, unitarity and coupling-constant perturbativity, and calculated the oblique parameters (S , T , U). Adopting the recent fit results in Ref. [24], we use the following values of S , T , U ,

$$S = 0.02 \pm 0.10, \quad T = 0.07 \pm 0.12, \quad U = 0.00 \pm 0.09. \quad (11)$$

The correlation coefficients are given by

$$\rho_{ST} = 0.89, \quad \rho_{SU} = 0.54, \quad \rho_{TU} = 0.83. \quad (12)$$

The oblique parameters favor that one of H and A has a small mass splitting from H^\pm , and therefore we simply take $m_A = m_{H^\pm}$ in this paper.

- (2) Muon $g - 2$. The model contributes to the muon $g - 2$ through the one-loop diagrams involving the μ - τ LFV coupling of H and A [17],

$$\delta a_\mu = \frac{m_\mu m_\tau \rho^2}{8\pi^2} \left[\frac{(\log \frac{m_H^2}{m_\tau^2} - \frac{3}{2})}{m_H^2} - \frac{\log(\frac{m_A^2}{m_\tau^2} - \frac{3}{2})}{m_A^2} \right]. \quad (13)$$

From Eq. (13), the model can give a positive contribution to the muon $g - 2$ for $m_A > m_H$. This is reason why we scan over the parameter space of $m_A > m_H$.

- (3) Lepton universality in the τ decays. The HFAG collaboration reported three ratios from pure leptonic processes, and two ratios from semi-hadronic processes, $\tau \rightarrow \pi/K\nu$ and $\pi/K \rightarrow \mu\nu$ [3]:

$$\begin{aligned} \left(\frac{g_\tau}{g_\mu}\right) &= 1.0011 \pm 0.0015, & \left(\frac{g_\tau}{g_e}\right) &= 1.0029 \pm 0.0015, & \left(\frac{g_\mu}{g_e}\right) &= 1.0018 \pm 0.0014, \\ \left(\frac{g_\tau}{g_\mu}\right)_\pi &= 0.9963 \pm 0.0027, & \left(\frac{g_\tau}{g_\mu}\right)_K &= 0.9858 \pm 0.0071, \end{aligned} \quad (14)$$

with

$$\begin{aligned}
\left(\frac{g_\tau}{g_\mu}\right)^2 &\equiv \bar{\Gamma}(\tau \rightarrow e\nu\bar{\nu})/\bar{\Gamma}(\mu \rightarrow e\nu\bar{\nu}), \\
\left(\frac{g_\tau}{g_e}\right)^2 &\equiv \bar{\Gamma}(\tau \rightarrow \mu\nu\bar{\nu})/\bar{\Gamma}(\mu \rightarrow e\nu\bar{\nu}), \\
\left(\frac{g_\mu}{g_e}\right)^2 &\equiv \bar{\Gamma}(\tau \rightarrow \mu\nu\bar{\nu})/\bar{\Gamma}(\tau \rightarrow e\nu\bar{\nu}).
\end{aligned} \tag{15}$$

Here $\bar{\Gamma}$ denotes the partial width normalized to its SM value. The correlation matrix for the above five observables is

$$\begin{pmatrix}
1 & +0.53 & -0.49 & +0.24 & +0.12 \\
+0.53 & 1 & +0.48 & +0.26 & +0.10 \\
-0.49 & +0.48 & 1 & +0.02 & -0.02 \\
+0.24 & +0.26 & +0.02 & 1 & +0.05 \\
+0.12 & +0.10 & -0.02 & +0.05 & 1
\end{pmatrix}. \tag{16}$$

In this model,

$$\begin{aligned}
\bar{\Gamma}(\tau \rightarrow \mu\nu\bar{\nu}) &= (1 + \delta_{\text{loop}}^\tau)^2 (1 + \delta_{\text{loop}}^\mu)^2 + \delta_{\text{tree}}, \\
\bar{\Gamma}(\tau \rightarrow e\nu\bar{\nu}) &= (1 + \delta_{\text{loop}}^\tau)^2, \\
\bar{\Gamma}(\mu \rightarrow e\nu\bar{\nu}) &= (1 + \delta_{\text{loop}}^\mu)^2.
\end{aligned} \tag{17}$$

Where δ_{tree} can give a positive correction to $\tau \rightarrow \mu\nu\bar{\nu}$, and is from the tree-level diagram mediated by the charged Higgs,

$$\delta_{\text{tree}} = 2 \frac{m_W^4 \rho^4}{g^4 m_{H^\pm}^4}. \tag{18}$$

$\delta_{\text{loop}}^\tau$ and δ_{loop}^μ denote the corrections to vertices $W\bar{\nu}_\tau\tau$ and $W\bar{\nu}_\mu\mu$, respectively, which are from the one-loop diagrams involving H , A , and H^\pm . Since we take $\rho_{\mu\tau} = \rho_{\tau\mu} \equiv \rho$, and therefore $\delta_{\text{loop}}^\tau = \delta_{\text{loop}}^\mu$. Following results of [10, 12, 22],

$$\delta_{\text{loop}}^\tau = \delta_{\text{loop}}^\mu = \frac{1}{16\pi^2} \rho^2 \left[1 + \frac{1}{4} (H(x_A) + H(x_H)) \right], \tag{19}$$

where $H(x_\phi) \equiv \ln(x_\phi)(1 + x_\phi)/(1 - x_\phi)$ with $x_\phi = m_\phi^2/m_{H^\pm}^2$.

In the model,

$$\left(\frac{g_\tau}{g_\mu}\right)_\pi = \left(\frac{g_\tau}{g_\mu}\right)_K = \left(\frac{g_\tau}{g_\mu}\right). \tag{20}$$

We perform χ^2_τ calculation for the five observables. The covariance matrix constructed from the data of Eq. (14) and Eq. (16) has a vanishing eigenvalue, and the corresponding degree is removed in our calculation.

- (4) Lepton universality in the Z decays. The measured values of the ratios of the leptonic Z decay branching fractions are given as [25]:

$$\frac{\Gamma_{Z \rightarrow \tau^+ \tau^-}}{\Gamma_{Z \rightarrow e^+ e^-}} = 1.0019 \pm 0.0032, \quad (21)$$

$$\frac{\Gamma_{Z \rightarrow \mu^+ \mu^-}}{\Gamma_{Z \rightarrow e^+ e^-}} = 1.0009 \pm 0.0028, \quad (22)$$

with a correlation of +0.63. The model can give corrections to the widths of $Z \rightarrow \tau^+ \tau^-$ and $Z \rightarrow \mu^+ \mu^-$ through the one-loop diagrams involving the extra Higgs bosons. The quantities of Eq. (21) are calculated in the model as [10, 12, 22]

$$\frac{\Gamma_{Z \rightarrow \tau^+ \tau^-}}{\Gamma_{Z \rightarrow e^+ e^-}} \approx 1.0 + \frac{2g_L^e \text{Re}(\delta g_L^{\text{loop}}) + 2g_R^e \text{Re}(\delta g_R^{\text{loop}})}{g_L^e{}^2 + g_R^e{}^2}. \quad (23)$$

where the SM value $g_L^e = -0.27$ and $g_R^e = 0.23$. δg_L^{loop} and δg_R^{loop} are from the one-loop corrections, which are given as

$$\delta g_L^{\text{loop}} = \frac{1}{8\pi^2} \rho^2 \left\{ -\frac{1}{2} B_Z(r_A) - \frac{1}{2} B_Z(r_H) - 2C_Z(r_A, r_H) + s_W^2 \left[B_Z(r_A) + B_Z(r_H) + \tilde{C}_Z(r_A) + \tilde{C}_Z(r_H) \right] \right\}, \quad (24)$$

$$\delta g_R^{\text{loop}} = \frac{1}{8\pi^2} \rho^2 \left\{ 2C_Z(r_A, r_H) - 2C_Z(r_{H^\pm}, r_{H^\pm}) + \tilde{C}_Z(r_{H^\pm}) - \frac{1}{2} \tilde{C}_Z(r_A) - \frac{1}{2} \tilde{C}_Z(r_H) + s_W^2 [B_Z(r_A) + B_Z(r_H) + 2B_Z(r_{H^\pm}) + \tilde{C}_Z(r_A) + \tilde{C}_Z(r_H) + 4C_Z(r_{H^\pm}, r_{H^\pm})] \right\}, \quad (25)$$

where $r_\phi = m_\phi^2/m_Z^2$ with $\phi = A, H, H^\pm$, and

$$B_Z(r) = -\frac{\Delta_\epsilon}{2} - \frac{1}{4} + \frac{1}{2} \log(r), \quad (26)$$

$$C_Z(r_1, r_2) = \frac{\Delta_\epsilon}{4} - \frac{1}{2} \int_0^1 dx \int_0^x dy \log[r_2(1-x) + (r_1-1)y + xy], \quad (27)$$

$$\begin{aligned} \tilde{C}_Z(r) &= \frac{\Delta_\epsilon}{2} + \frac{1}{2} - r[1 + \log(r)] + r^2[\log(r) \log(1+r^{-1}) \\ &\quad - \text{Li}_2(-r^{-1})] - \frac{i\pi}{2} [1 - 2r + 2r^2 \log(1+r^{-1})]. \end{aligned} \quad (28)$$

Due to $\rho_{\mu\tau} = \rho_{\tau\mu} \equiv \rho$, we can obtain

$$\frac{\Gamma_{Z \rightarrow \mu^+ \mu^-}}{\Gamma_{Z \rightarrow e^+ e^-}} = \frac{\Gamma_{Z \rightarrow \tau^+ \tau^-}}{\Gamma_{Z \rightarrow e^+ e^-}}. \quad (29)$$

(5) The exclusions from the ATLAS and CMS searches at the LHC. The extra Higgs bosons are dominantly produced at the LHC via the following electroweak processes:

$$pp \rightarrow W^{\pm*} \rightarrow H^{\pm} A, \quad (30)$$

$$pp \rightarrow Z^* \rightarrow H A, \quad (31)$$

$$pp \rightarrow W^{\pm*} \rightarrow H^{\pm} H, \quad (32)$$

$$pp \rightarrow Z^* / \gamma^* \rightarrow H^+ H^-. \quad (33)$$

For small mass splitting among H , A , and H^{\pm} , the dominant decay modes of these Higgses are

$$H \rightarrow \tau^{\pm} \mu^{\mp}, \quad A \rightarrow \tau^{\pm} \mu^{\mp}, \quad H^{\pm} \rightarrow \tau^{\pm} \nu_{\mu}, \mu^{\pm} \nu_{\tau}. \quad (34)$$

When m_A and $m_{H^{\pm}}$ are much larger than m_H , the following exotic decay modes will open with $m_A = m_{H^{\pm}}$,

$$A \rightarrow H Z, \quad H^{\pm} \rightarrow H W^{\pm}. \quad (35)$$

In order to restrict the productions of the above processes at the LHC for our model, we perform simulations for the samples using `MG5_aMC-2.4.3` [26] with `PYTHIA6` [27] and `Delphes-3.2.0` [28], and adopt the constraints from all the analysis for the 13 TeV LHC in version `CheckMATE 2.0.26` [29]. Besides, the latest multi-lepton searches for electroweakino [30–34] implemented in Ref. [35] and the ATLAS search for direct stau production with 139 fb^{-1} 13 TeV events [36] are also taken into consideration.

B. Results and discussions

We find that the constraints from theory, oblique parameters and Z decays can be easily satisfied in the parameter space taken in this paper. The allowed ranges of m_H , m_A , $m_{H^{\pm}}$, and ρ are not reduced by the those constraints. Therefore, we won't show their results in the following discussions.

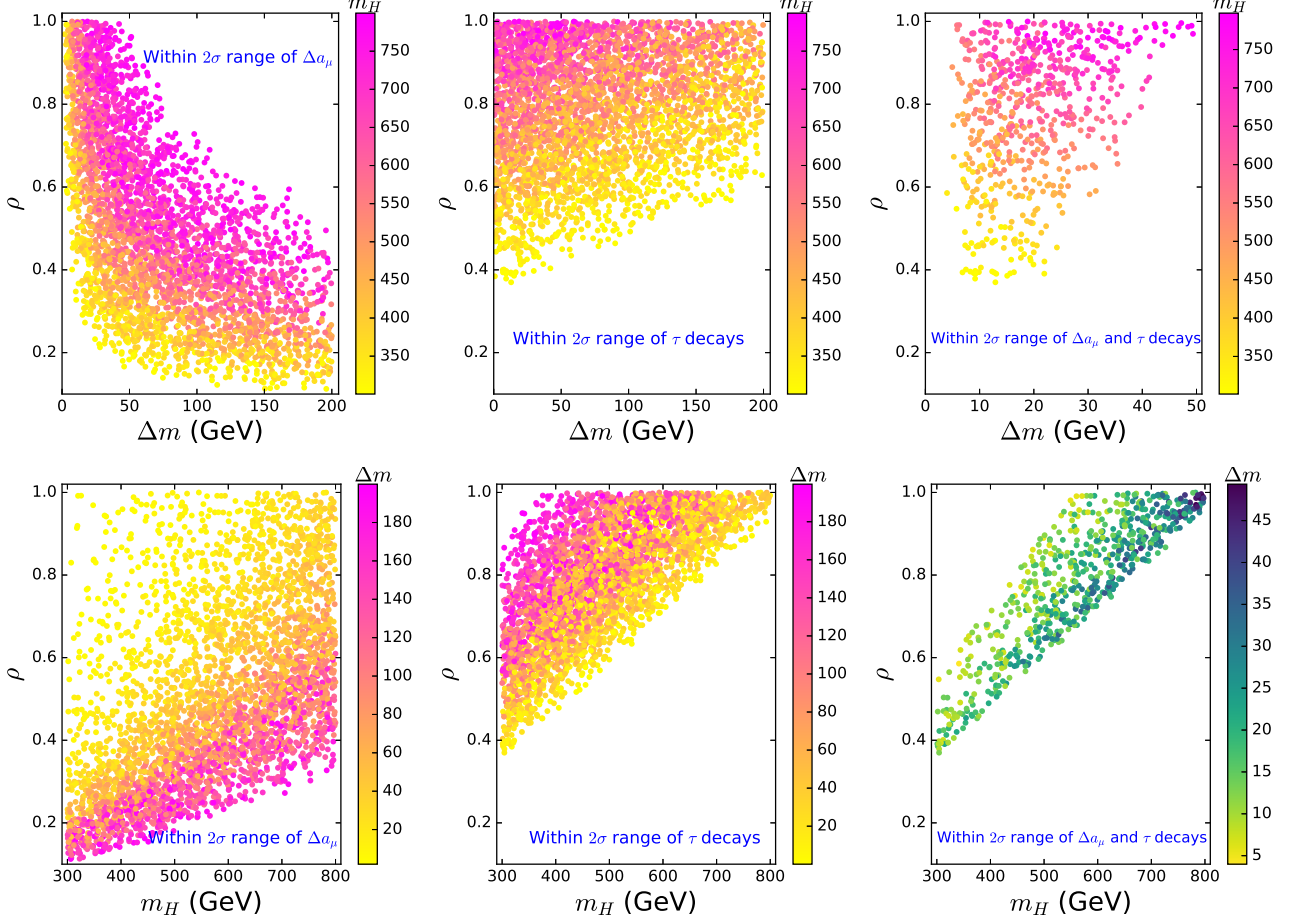


FIG. 1: The samples within 2σ ranges of Δa_μ (left panel), LUF in the τ decays (middle panel), and both Δa_μ and LUF in the τ decays (right panel). All the samples satisfy the constraints of the theory, oblique parameters and Z decays. Here $\Delta m \equiv m_A(m_{H^\pm}) - m_H$.

After imposing the constraints of the theory, the oblique parameters, and Z decays, in Fig. 1 we show the surviving samples which are consistent with Δa_μ and τ decays at 2σ level. The contributions of H and A to Δa_μ are respectively positive and negative, and a large mass splitting between m_A and m_H can produce sizable corrections to Δa_μ . Thus, with an increase of Δm , a relative small ρ can make Δa_μ to be within 2σ range of experimental data, as shown in upper-left panel in Fig. 1.

The experimental value of $\left(\frac{g_\tau}{g_e}\right)$ has about 2σ positive deviation from the SM prediction. Enhancement of $\Gamma(\tau \rightarrow \mu\nu\bar{\nu})$ can provide a better fit. According to Eq. (17), the δ_{tree} term can enhance $\Gamma(\tau \rightarrow \mu\nu\bar{\nu})$, and favor ρ to increase with m_{H^\pm} , see Eq. (18). Therefore, the upper-middle panel shows that the experimental data of LFU in the τ decays favor ρ to

increase with Δm . Because of the opposite relationship between ρ and Δm , the excesses of Δa_μ and τ decays can be simultaneously explained in a narrow region of ρ and Δm . As shown in the upper-right panel, $\Delta m < 50$ GeV and $\rho > 0.36$ are required, and ρ is favored to increase with Δm .

The lower panels of Fig. 1 show that the experimental data of Δa_μ and τ decays favor ρ to increase with m_H . The lower-right panel shows that the excesses of Δa_μ and τ decays can be simultaneously explained in the range of $300 \text{ GeV} < m_H < 800 \text{ GeV}$, and the corresponding ρ is imposed upper and lower bounds. Taking $m_H = 500 \text{ GeV}$ for an example, the excesses of Δa_μ and LUF in the τ decays can be simultaneously explained for $0.6 < \rho < 0.9$. For $m_H = 500 \text{ GeV}$ and $\rho < 0.6$, Δa_μ can be explained, but the τ decays can not be accommodated. For $m_H = 500 \text{ GeV}$ and $\rho > 0.9$, Δa_μ and the τ decays can be respectively explained. However, the former favors a small Δm and the latter favors a large Δm , which leads that the two anomalies can not be simultaneously explained for $m_H = 500 \text{ GeV}$ and $\rho > 0.9$.

After imposing the constraints of the direct searches at the LHC, those samples of Fig. 1 are projected on the planes of m_H versus ρ and m_H versus Δm , as shown in Fig. 2. Since the excesses of Δa_μ and τ decays require the mass splitting between m_A (m_{H^\pm}) and m_H to be smaller than 50 GeV, H , A and H^\pm will dominantly decay into $\tau\mu$, $\tau\nu_\mu$, and $\mu\nu_\tau$. The direct searches at the LHC exclude region of $m_H < 560 \text{ GeV}$, and the corresponding ρ is required to be larger than 0.68. Since Δm is such small, it hardly affects the excluded region.

For the excluded samples, the most sensitive experimental analysis is the CMS search for electroweak production of charginos and neutralinos in multilepton final states [32] at 13 TeV LHC with 35.9 fb^{-1} integrated luminosity data. In this analysis, hundreds of signal region bins are designed, of which the **SR-A44** and **SR-C18** provide strongest constraints on our samples. In the **SR-A44**, events are selected on the condition that contain three leptons that form at least one opposite-sign same-flavor (OSSF) pair, $M_{\ell\ell} > 105 \text{ GeV}$, $p_T^{\text{miss}} > 200 \text{ GeV}$ and $M_T > 160 \text{ GeV}$. Here $M_{\ell\ell}$ is the invariant mass of the OSSF dilepton pair, p_T^{miss} stands the missing transverse momentum, and $M_T = \sqrt{2p_T^{\text{miss}}p_T^\ell[1 - \cos(\Delta\phi)]}$ is the transverse mass computed with respect to the third lepton in the event. The **SR-C** is built from events with two e or μ forming an OSSF pair and a hadronic decay tau lepton τ_h . The bin **SR-C18** requires $p_T^{\text{miss}} > 200 \text{ GeV}$, $|M_{\ell\ell} - m_Z| > 15 \text{ GeV}$ and $M_{T2} > 100 \text{ GeV}$. The

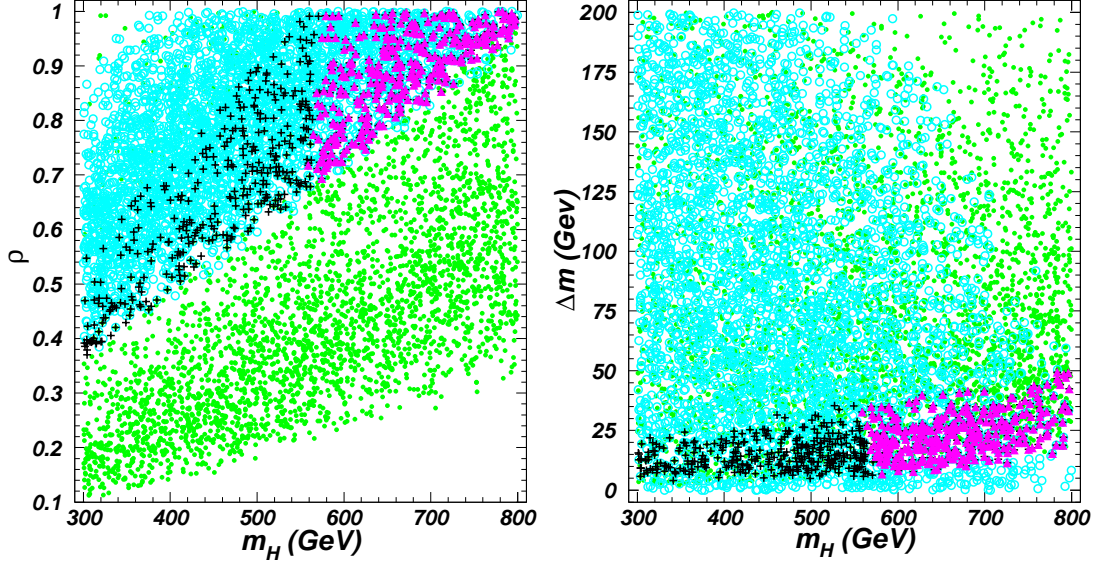


FIG. 2: The surviving samples on the planes of m_H versus ρ and m_H versus Δm . All the samples satisfy the constraints of the theory, oblique parameters and Z decays. In addition, the bullets (green) within the 2σ ranges of muon $g-2$ and the circles (blue) within the 2σ ranges of LUF in the τ decays. The pluses (black) and triangles (purple) are within the 2σ ranges of both muon $g-2$ and LUF in the τ decays, and the former are excluded by the constraints of the direct searches at the LHC, while the latter are allowed.

two-lepton transverse mass M_{T2} [37, 38] is computed with the OSSF pair of light leptons. The main contributions of our samples to the bins are from processes in Eq. (30,32) with one or two of the τ s decaying hadronically. Thus, the exclusion power decreases gently with heavier m_H and M_A due to the smaller production rates for the processes, as shown in the left panel of Fig. 3.

We also adopt the ATLAS search for direct stau production with 139 fb^{-1} integrated luminosity data at 13 TeV LHC [36]. Although the integrated luminosity is much higher than the multilepton search [32], the stau search can not constrain any sample with $m_H > 300 \text{ GeV}$. We can see from the left panel of Fig. 3 that the largest R-value, the ratio of event yields in signal region to the corresponding 95% experimental limit, is 0.24 for our samples. It is because that both the signal regions of the stau search [36], **SR-lowMass** and **SR-highMass**, require exactly two taus with opposite-sign electric charge, and reject events with an additional third τ or light lepton. So only process in Eq. (33) could contribute to the signal regions. The other searches corresponding to an integrated luminosity of 139 fb^{-1}

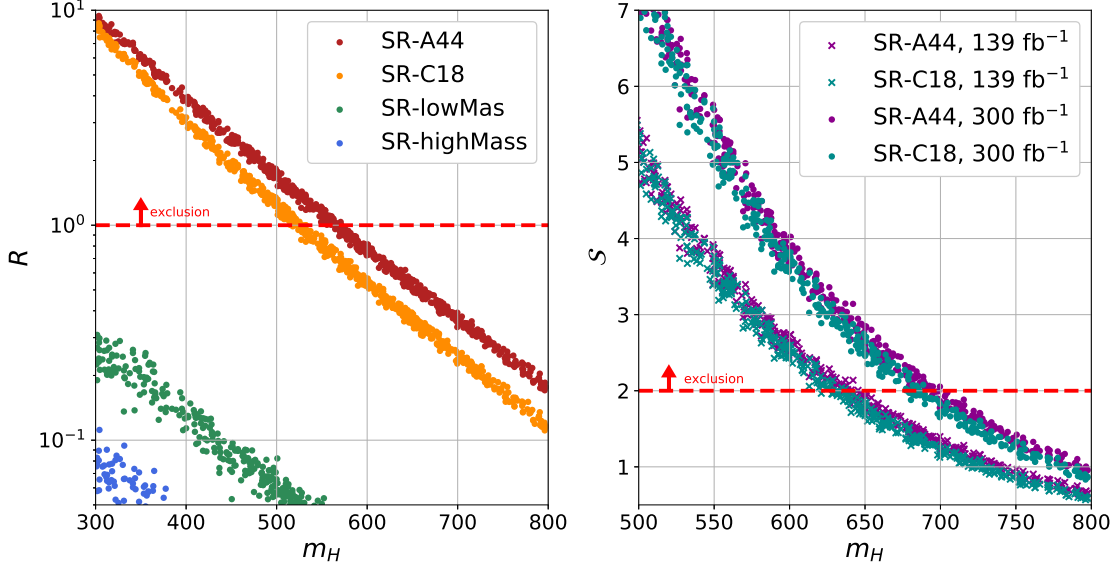


FIG. 3: Left panel: the ratio R of event yields in the signal regions to the corresponding 95% experimental limit for the surviving samples. The red and orange dots represent the signal regions SR-A44 and SR-C18 of the multilepton search with 35.9 fb $^{-1}$ LHC data [32]. The green and blue dots stand the signal regions SR-lowMass and SR-highMass of the stau search with 139 fb $^{-1}$ LHC data [36]. Right panel: the estimated expected significance S for the surviving sample with high integrated luminosity. The purple and cyan dots stand the signal regions SR-A44 and SR-C18 with 139 fb $^{-1}$ integrated luminosity data (crosses) and 300 fb $^{-1}$ integrated luminosity data (dots).

face the similar issues, such as requiring multiple jets [39–41], hard jet [42, 43], b-tagged jet [44], or exactly two light flavor leptons [42, 45].

Given the fact that hundred of integrated luminosity 13 TeV events have been recorded at LHC, we further estimate the exclusion power of LHC with higher luminosity by normalizing signal and background event yields in the signal regions SR-A44 and SR-C18 of [32]. We compute the significance as $S = \sqrt{2(n_s + n_b) \ln(1 + n_s/n_b) - 2n_s}$, where n_s and n_b are the normalized signal and background event yields, respectively. We show the result in the right panel of Fig. 3. The samples with $m_H < 645$ (700) GeV will be excluded at 2σ confidence level with 139 (300) fb $^{-1}$ integrated luminosity data. If the signal regions of [32] are optimized for the production and decay modes in Eq. (30-34), the detection ability of LHC for this model could be further enhanced.

IV. CONCLUSION

In this paper, we proposed a 2HDM in which one Higgs doublet has the same interactions with fermions as the SM, and another Higgs doublet only has the μ - τ LFV interactions. Assuming the Yukawa matrices to be real and symmetric, we considered various relevant theoretical and experimental constraints, and found that the excesses of muon $g - 2$ and LUF in the τ decays can be simultaneously explained in many parameter spaces with $300 \text{ GeV} < m_H < 800 \text{ GeV}$, $\Delta m < 50 \text{ GeV}$, and $0.36 < \rho < 1$. The parameter spaces are sizable reduced by the direct search limits from the LHC, and m_H is required to be larger than 560 GeV.

Note added: When this manuscript is being prepared, a similar paper appeared in the arXiv [46]. Here we discussed different scenario, and obtain different conclusions.

Acknowledgment

This work was supported by the Natural Science Foundation of Shandong province (ZR2017JL002 and ZR2017MA004), by the National Natural Science Foundation of China under grant 11575152, and by the ARC Centre of Excellence for Particle Physics at the Tera-scale under the grant CE110001004.

-
- [1] H. N. Brown et al. [Muon g-2 Collaboration], Phys. Rev. Lett. **86**, (2001) 2227.
 - [2] T. Blum et al. [RBC and UKQCD Collaborations], Phys. Rev. Lett. **121**, (2018) 022003.
 - [3] Y. Amhis et al. [Heavy Flavor Averaging Group (HFAG) Collaboration], arXiv:1412.7515.
 - [4] D. Chang, W.-F. Chang, C.-H. Chou, and W.-Y. Keung, Phys. Rev. D **63**, (2001) 091301.
 - [5] K. M. Cheung, C. H. Chou and O. C. W. Kong, Phys. Rev. D **64**, (2001) 111301.
 - [6] K. Cheung and O. C. W. Kong, Phys. Rev. D **68**, (2003) 053003.
 - [7] J. Cao, P. Wan, L. Wu and J. M. Yang, Phys. Rev. D **80**, (2009) 071701.
 - [8] A. Broggio, E. J. Chun, M. Passera, K. M. Patel and S. K. Vempati, JHEP **1411**, (2014) 058.
 - [9] L. Wang and X. F. Han, JHEP **05**, (2015) 039.
 - [10] T. Abe, R. Sato and K. Yagyu, JHEP **1507**, (2015) 064.

- [11] E. J. Chun, Z. Kang, M. Takeuchi, Y.-L. Tsai, JHEP **1511**, (2015) 099.
- [12] E. J. Chun, J. Kim, JHEP **1607**, (2016) 110.
- [13] A. Crivellin, J. Heeck, P. Stoffer, Phys. Rev. Lett. **116**, (2016) 081801.
- [14] L. Wang, J. M. Yang, M. Zheng, Y. Zhang, Phys. Lett. B **788**, (2019) 519-529.
- [15] X.-F. Han, T. Li, L. Wang, Y. Zhang, Phys. Rev. D **99**, (2019) 095034.
- [16] K. Adikle Assamagan, A. Deandrea, P.-A. Delsart, Phys. Rev. D **67**, (2003) 035001.
- [17] S. Davidson, G. J. Grenier, Phys. Rev. D **81**, (2010) 095016.
- [18] Y. Omura, E. Senaha, K. Tobe, JHEP **1505**, (2015) 028.
- [19] R. Benbrik, C.-H. Chen, T. Nomura, Phys. Rev. D **93**, (2016) 095004.
- [20] Y. Omura, E. Senaha, K. Tobe, Phys. Rev. D **94**, (2016) 055019.
- [21] L. Wang, S. Yang, X.-F. Han, Nucl. Phys. B **919**, (2017) 123-141.
- [22] Y. Abe, T. Toma, K. Tsumura, JHEP **1906**, (2019) 142.
- [23] D. Eriksson, J. Rathsmann, O. Stål, Comput. Phys. Commun. **181**, (2010) 189.
- [24] M. Tanabashi et al., [Particle Data Group], Phys. Rev. D **98**, 030001 (2018).
- [25] S. Schael et al. [ALEPH and DELPHI and L3 and OPAL and SLD and LEP Electroweak Working Group and SLD Electroweak Group and SLD Heavy Flavour Group Collaborations], Phys. Rept. **427**, (2006) 257.
- [26] J. Alwall *et al.*, JHEP **1407**, (2014) 079.
- [27] P. Torrielli and S. Frixione, JHEP **1004**, (2010) 110.
- [28] J. de Favereau *et al.* [DELPHES 3 Collaboration], JHEP **1402**, (2014) 057.
- [29] D. Dercks, N. Desai, J. S. Kim, K. Rolbiecki, J. Tattersall and T. Weber, Comput. Phys. Commun. **221**, (2017) 383.
- [30] A. M. Sirunyan *et al.* [CMS Collaboration], JHEP **1711**, (2017) 029.
- [31] A. M. Sirunyan *et al.* [CMS Collaboration], JHEP **1803**, (2018) 076.
- [32] A. M. Sirunyan *et al.* [CMS Collaboration], JHEP **1803**, (2018) 166.
- [33] A. M. Sirunyan *et al.* [CMS Collaboration], JHEP **1803**, (2018) 160.
- [34] M. Aaboud *et al.* [ATLAS Collaboration], Eur. Phys. J. C **78**, (2018) 154.
- [35] G. Pozzo and Y. Zhang, Phys. Lett. B **789**, (2019) 582-591.
- [36] The ATLAS collaboration [ATLAS Collaboration], ATLAS-CONF-2019-018.
- [37] C. G. Lester and D. J. Summers, Phys. Lett. B **463**, 99 (1999).
- [38] A. Barr, C. Lester and P. Stephens, J. Phys. G **29**, 2343 (2003).

- [39] CMS Collaboration [CMS Collaboration], CMS-PAS-SUS-19-008.
- [40] CMS Collaboration [CMS Collaboration], CMS-PAS-SUS-19-003.
- [41] The ATLAS collaboration [ATLAS Collaboration], ATLAS-CONF-2019-015.
- [42] The ATLAS collaboration [ATLAS Collaboration], ATLAS-CONF-2019-014.
- [43] The ATLAS collaboration [ATLAS Collaboration], ATLAS-CONF-2019-020.
- [44] The ATLAS collaboration [ATLAS Collaboration], ATLAS-CONF-2019-031.
- [45] The ATLAS collaboration [ATLAS Collaboration], ATLAS-CONF-2019-008.
- [46] S. Iguro, Y. Omura, M. Takeuchi, arXiv:1907.09845.